Macromolecules

Article

pubs.acs.org/Macromolecules

Thermally Cross-Linked Anion Exchange Membranes from Solvent Processable Isoprene Containing Ionomers

Tsung-Han Tsai,[†] S. Piril Ertem,[†] Ashley M. Maes,[‡] Soenke Seifert,[§] Andrew M. Herring,[‡] and E. Bryan Coughlin*[,†]

[†]Department of Polymer Science and Engineering, University of Massachusetts Amherst, 120 Governors Drive, Amherst, Massachusetts 01003, United States

[‡]Department of Chemical and Biological Engineering, Colorado School of Mines, Golden, Colorado 80401, United States

[§]X-ray Science Division, Argonne National Laboratory, Argonne, Illinois 60439, United States

Supporting Information

ABSTRACT: Random copolymers of isoprene and 4-vinylbenzyl chloride (VBCl) with varying compositions were synthesized via nitroxide-mediated polymerization. Subsequent quaternization afforded solvent processable and cross-linkable ionomers with a wide range of ion exchange capacities (IECs). Solution cast membranes were thermally cross-linked to form anion exchange membranes. Cross-linking was achieved by taking advantage of the unsaturations on the polyisoprene backbone, without added cross-linkers. A strong correlation was found between water uptake and ion conductivity of the membranes: conductivities of the membranes with IECs beyond a critical value were found to be constant related to their high water absorption. Environmentally controlled small-angle X-ray scattering experiments revealed a correlation between the average distance between ionic clusters and the ion conductivity, indicating that a well-connected network of ion clusters is necessary for efficient ion conduction and high ion conductivity.

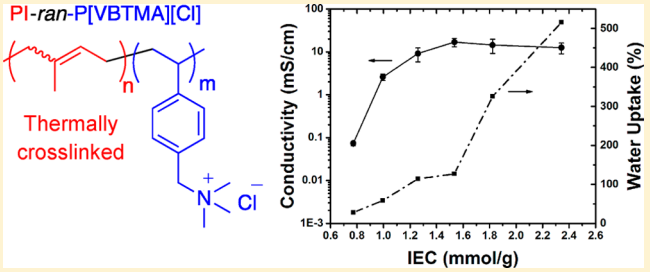

INTRODUCTION

Anion exchange membranes (AEMs) are attracting renewed interest over the past decade as an alternative to proton exchange membranes (PEMs) for fuel cell applications. AEM fuel cells offer several advantages over PEM fuel cells.[1−3] One of the major advantages are the faster electrokinetics under alkaline conditions for oxygen reduction and fuel oxidation reactions at the electrodes. This allows utilization of non-noble-metal catalysts as electrode materials, thus reducing cost. Moreover, more facile oxidation of low-carbon alcohols provides a broader choice of fuels with high volumetric energy density for energy conversion.

When designing optimized AEMs, it is important to achieve certain key requirements: high ion conductivity (>100 mS/cm), mechanical durability, and chemical stability. The lower mobility of hydroxide ion compared to proton requires a higher charge carrier density in AEMs. Therefore, high ion exchange capacities (IECs) are necessary to achieve comparable conductivities to PEMs. However, mechanical properties are usually compromised at high IEC values due to excessive water absorption and swelling. This trade-off between mechanical durability and ion conductivity creates a need for new methods to improve mechanical integrity without compromising ion conductivity.

Cross-linking has shown to be a useful approach to generate robust materials. Several methods have been used to fabricate water insoluble mechanically robust membranes. One method is cross-linking through quaternization. For example, Varcoe et al. prepared cross-linked AEMs from reacting poly(vinyl benzyl chloride) (PVBCl) with 1,6-hexanediamine.[4] When chloromethylated polysulfones were quaternized with alkyldiamines, membranes with improved mechanical integrities, chemical stabilities, and acceptable ionic conductivities were obtained.[5−8]

Another approach is to insert quaternized moieties into a network structure. A quaternary ammonium functionalized epoxide was used to cross-link poly(vinyl alcohol).[9] Functionalized cyclic alkenes were used to form cross-linked AEMs by ring-opening metathesis polymerization. Robertson et al. have developed a network structure using a quaternary ammonium functionalized cyclooctene cross-linker.[10] These membranes were optimized to exhibit good mechanical stability and high ion conductivity (111 mS/cm, OH^-; 26.4 mS/cm, Cl^-, at 50 °C in water). Quaternary ammonium functionalized norbornenes were designed by Clark et al. (28 mS/cm, OH^-, at 50 °C in water)[11] while Zha et al.[12] developed ruthenium cation attached norbornenes to form cross-linked networks (28.6 mS/cm, OH^-, at 30 °C in water). Recently, Price et al. studied a network using a poly(vinylbenzyltrimethylammonium) precur-

Received: November 21, 2014
Revised: January 15, 2015
Published: January 28, 2015

DOI: 10.1021/ma502362a
Macromolecules 2015, 48, 655−662

sor with norbornene pendent groups.[13] Cross-linking this precursor with cyclic alkenes yielded an AEM with a bicontinuous morphology and high ionic conductivity (120 mS/cm, OH^-, at 60 °C in water).

In most of these cases cross-linking takes place during membrane casting, which eliminates the possibility of solvent processing, and thus less control over membrane fabrication. Solvent processability is also desired for producing high performance membrane electrode assemblies by infusing the ionomers into electrocatalyst layers.[4,14] In all of the above-mentioned cases an added cross-linker was used. There are only a few AEMs that can be prepared from solvent processable materials that allow cross-linking after membrane casting without addition of cross-linkers. Coates et al. designed tetraalkylammonuim-functionalized polyethylene-like polymers.[14] While these polymers were soluble in aqueous *n*-propanol, they were insoluble in water at optimized IECs due to physical cross-linking imparted by the polyethylene-like backbone. Gu et al. used quaternary phosphonium containing polysulfones and cross-linked the membranes by thermal treatment after membrane casting using Friedel−Crafts alkylation chemistry.[15] Recently, Wang and Hickner reported low-temperature cross-linking of styrene-based copolymers with pendent alkenes via olefin metathesis reactions.[16]

Here, we designed random copolymers of vinylbenzyltrimethylammonium (VBTMA) and isoprene that are solvent processable and cross-linkable. The isoprene units formed a basis for the rubbery hydrophobic matrix. Robust, flexible, and ion conducting membranes were obtained through a simple thermal treatment by taking advantage of the unsaturations on the hydrocarbon backbone without addition of any extra cross-linkers or initiators. Ion conductivity of the membranes was investigated and compared with their water uptake properties. Small-angle X-ray scattering (SAXS) experiments under controlled humidity and temperature were employed to correlate structure with conductivity.

EXPERIMENTAL SECTION

Materials. Isoprene (99%, Alfa Aesar) was distilled under nitrogen prior to use. 4-Vinylbenzyl chloride (VBCl) (90%, Acros Organics) was passed through a column of basic alumina. 4,5-Bis(1,1-dimethylethyl)-6-ethoxy-2,2-dimethyl-3,7-dioxa-4-aza-6-phosphanonanoic acid 6-oxide (SG1) (BlockBuilder) were kindly provided by Arkema. Other chemicals were used as received.

General Synthetic Procedure for Polyisoprene-*ran*-Poly(vinylbenzyl chloride) (PI-*ran*-PVBCl) Copolymers. All of the PI-*ran*-PVBCl copolymers were synthesized following a similar procedure. A representative experimental procedure is as follows: isoprene (8.17 g, 119.96 mmol), vinylbenzyl chloride (6.28 mg, 41.16 mmol), and SG1 (21 mg, 54.3 μmol) were weighed into a Teflon-sealed Schlenk flask equipped with a magnetic stirrer. The mixture was degassed by three freeze−pump−thaw cycles and subsequently refilled with nitrogen gas. The copolymerization was performed at 125 °C for 20 h. The reaction was quenched by immersing the flask into an ice bath. The reaction mixture was diluted with dichloromethane and was recovered by twice precipitating in methanol.

General Procedure for Quaternization. PI-*ran*-PVBCl precursor (about 1 g) was added into a vial containing 16 mL of 50 wt % trimethylamine aqueous solution. The quaternization reaction was performed at 60 °C for 16 h. During the reaction the PI-*ran*-PVBCl copolymers became water-soluble. After the reaction water was removed by evaporation—first under air flow and then under reduced pressure at 40 °C for 20 h. The quaternized polymer polyisoprene-*ran*-poly(vinylbenzyltrimethylammonium chloride) (PI-*ran*-P[VBTMA][Cl]) was obtained as pale yellow solid. The quaternized polymers are denoted as PI-*ran*-P[VBTMA][Cl]-*x*, where *x* is the ion exchange capacity (IEC) of the polymer. Quaternized polymers were stored at −30 °C in the dark until used.

Membrane Fabrication and Thermal Cross-Linking Procedure. Membranes were fabricated by drop-casting a methanol solution of desired PI-*ran*-P[VBTMA][Cl] precursor (10 wt %) onto a Teflon sheet. The cast solutions were covered with a glass Petri dish to allow slow drying at ambient condition for 24 h. Membranes were further dried under vacuum at room temperature for 24 h. The dried membranes were thermally cross-linked in a preheated oven at 145 °C for a desired time interval. Membranes with a nominal thickness around 0.2 mm were obtained.

Characterizations. ^{1}H NMR spectroscopy was performed on a Bruker DPX-300 FT-NMR. Gel permeation chromatography (GPC) was performed in THF at a flow rate of 1.0 mL/min using a refractive index detector on a Polymer Laboratories PL-GPC 50 Integrated GPC system. The molecular weights reported are calculated against polystyrene standards. Infrared spectroscopy was performed on a PerkinElmer Spectrum 100 FTIR spectrometer with universal ATR sampling accessory. Thermal gravimetrical analysis (TGA) was conducted under air with TGA Q500 from TA Instruments. A 5−10 mg sample was first equilibrated at 25 °C and then heated to 700 °C with a temperature ramp rate of 10 °C/min. For isothermal TGA the sample was heated to 145 °C with a temperature ramp rate of 10 °C/min. The sample was heated at constant temperature for 12 h. The in-plane conductivity was analyzed using electrochemical impedance spectroscopy (EIS) to measure membrane resistance. The membrane was mounted in a four-electrode test cell, with platinum electrodes that are separated by a constant distance *L*. Impedance spectra were obtained over a frequency range of 1 Hz to 10 kHz. EIS data were collected using a Bio-Logic VMP3 potentiostat. Chloride conductivity measurements were made while the sample was in a TestEquity H1000 oven to control temperature and relative humidity (RH). At each RH studied, the temperature was varied from 50 to 90 °C by steps of 10 °C. Samples were allowed to equilibrate at each temperature set point for 35 min before data were collected. Data were collected and analyzed using EC Laboratories software. Equation 1 is used to relate conductivity to resistance.

$$\sigma = \frac{L}{Rwt} \tag{1}$$

where *R* is the membrane polarization resistance, *L* is the distance between the electrodes, *w* is the width of the membrane samples, and *t* is the thickness of the sample.

Small-angle X-ray scattering (SAXS) experiments were performed at the Advanced Photon Source at Argonne National Laboratory on beamline 12 ID-B. A Pliatus 2 M SAXS detector was used to collect scattering data from the X-ray beam at a wavelength of 1 Å and power of 12 keV with an acquisition time of 1 s. Intensity (I) is analyzed from the radial integration of the 2D scattering pattern with respect to the scattering vector (q). Temperature and humidity of the sample environment during scattering measurements were controlled with a custom-designed oven with four sample slots, as described previously.[17,18] Humidity of the oven was controlled using a combination of saturated and dry nitrogen streams. In a typical experiment three membranes and one empty sample holder were loaded so that a background spectrum of the environment and Kapton windows were collected for each experimental condition. Spectra were analyzed after background subtraction for the corresponding experimental condition. Samples were kept in water prior to loading. After removing the membranes from water, the samples were lightly dried with a KimWipe, mounted onto sample holders with Kapton tape, and loaded into the oven at 60 °C at dry conditions. Loaded samples were allowed to dry for 20 min under dry gas flow. The temperature was kept constant as the RH was increased to 95% RH. Samples were allowed to equilibrate for 60 min at 95% RH before X-ray measurement.

Ion exchange capacity (IEC) is defined as number of charged groups per gram of polymer and was calculated from the ratio of VBCl to isoprene determined by ^{1}H NMR of each copolymer. Hydration

DOI: 10.1021/ma502362a
Macromolecules 2015, 48, 655−662

Scheme 1. Polymerization of Isoprene and VBCl via Nitroxide-Mediated Polymerization To Form PI-*ran*-PVBCl

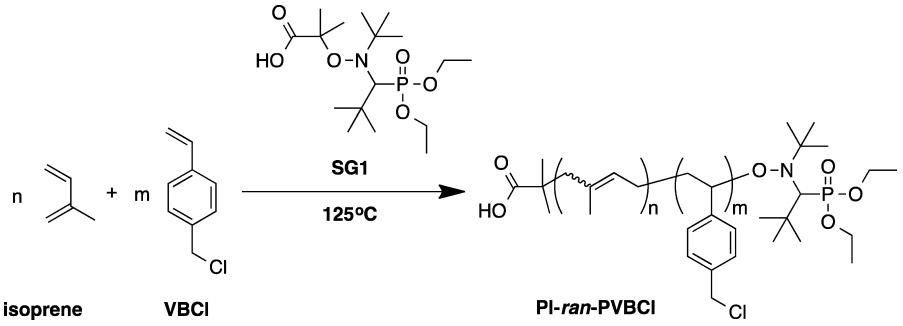

Table 1. PI-*ran*-PVBCl Copolymers, Their Molecular Weight, Dispersity and Copolymer Composition, and IEC of PI-*ran*-P[VBTMA][Cl]-*x* after Quaternization

	PI-*ran*-PVBCl				PI-*ran*-P[VBTMA][Cl]
PI-*ran*-P[VBTMA][Cl]-*x*	M_n[a] (kg/mol)	$Đ$[a]	f_{VBCl} ^{1}H NMR[b] (%)	f_{VBCl} feed[c] (%)	IEC[d] (mmol/g)
PI-*ran*-P[VBTMA][Cl]-0.77	77.4	1.94	5.9	5.0	0.77
PI-*ran*-P[VBTMA][Cl]-1.00	64.7	2.64	7.9	10	1.00
PI-*ran*-P[VBTMA][Cl]-1.26	111.0	2.88	10.5	11.5	1.26
PI-*ran*-P[VBTMA][Cl]-1.54	67.3	3.29	14.0	15	1.54
PI-*ran*-P[VBTMA][Cl]-1.82	73.4	3.21	16.8	20	1.82
PI-*ran*-P[VBTMA][Cl]-1.96	82.6	2.82	18.5	20	1.96
PI-*ran*-P[VBTMA][Cl]-2.34	105.3	2.18	24.0	25	2.34

[a]M_n and $Đ$ of PI-*ran*-PVBCl were measured by GPC versus narrow linear PS standards. [b]Mole percent of VBCl as analyzed by ^{1}H NMR. [c]Mole percent of VBCl in the monomer feed. [d]IEC was calculated based on the mole percent of VBCl as analyzed by ^{1}H NMR.

Scheme 2. Quaternization of PI-*ran*-PVBCl To Form PI-*ran*-P[VBTMA][Cl] Ionomers

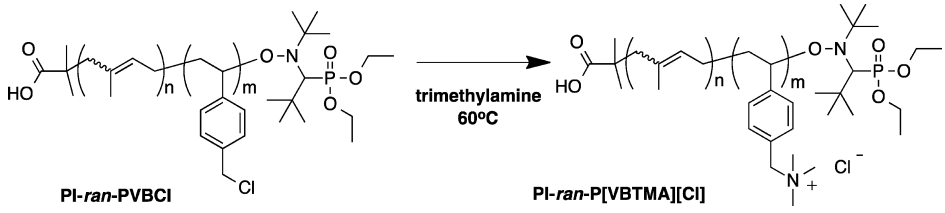

number (λ) is a measure of the number of water molecules per charged moiety; this value was calculated from the equation

$$\lambda = \frac{\mathrm{WU}}{\mathrm{MW_{water}} \times \mathrm{IEC}} \quad (2)$$

Here WU stands for the water uptake, defined as the weight ratio of absorbed water to the weight of dry membranes, and was calculated by the equation

$$\mathrm{WU} = \frac{m_{wet} - m_{dry}}{m_{dry}} \times 100 \quad (3)$$

Dry mass m_{dry} of the membranes was determined after drying membranes for 24 h under reduced pressure. For m_{wet}, membranes were soaked in water for 24 h. Before weighing, the surface of the membranes was gently wiped to remove excess water.

RESULTS AND DISCUSSION

Synthesis and Characterization of PI-*ran*-P[VBTMA][Cl]-*x* Copolymers. Precursor copolymers of PI-*ran*-PVBCl were synthesized through nitroxide-mediated polymerization (NMP), a versatile technique suitable for polymerization of a wide range of monomers.[19−21] NMP is compatible with many functional groups allowing copolymerization of 1,3-dienes with various styrenic and methacrylic monomers.[22] Compared to conventional free radical polymerization, NMP allows synthesis of high average molecular weight polyisoprene.[23]

Varying compositions of the PI-*ran*-PVBCl precursors were obtained by adjusting the molar ratio of isoprene to 4-vinylbenzyl chloride (VBCl) in the copolymerization reaction (Scheme 1). Copolymer compositions were determined from ^{1}H NMR by comparing the corresponding integrals of the resonances of the vinylic protons of the isoprene units to the benzylic protons of the VBCl units (Table 1 and Figure S1). The random character of the PI-*ran*-PVBCl copolymers was confirmed by matching the values of the monomer feed ratio and the analyzed copolymer compositions. Reactivity ratios of isoprene and VBCl (1.30 and 0.75, respectively) estimated from their Q−e values further support the random character of the synthesized copolymers.[24]

Molecular weight analysis of the synthesized PI-*ran*-PVBCl copolymers showed moderate to high number-average molecular weights and rather broad molecular weight dispersities (Table 1). While NMP is a controlled radical polymerization technique, moderate molecular weight control has been reported for homopolymerization of isoprene under similar reaction conditions.[21] The broad dispersities are indicative of possible chain transfer reactions during polymerization, resulting in nonuniform molecular weights and

DOI: 10.1021/ma502362a
Macromolecules 2015, 48, 655−662

presumably also nonlinear architectures. Since these copolymers were designed to form covalently cross-linked network structures, for the purposes of this work a well-controlled molecular weight and linear architecture are not crucial.

PI-*ran*-PVBCl precursor copolymers were quaternized by the reaction of the random copolymers with excess trimethylamine (TMA). The benzyl chloride groups were quantitatively converted into benzyltrimethylammonium (BTMA) cations to obtain PI-*ran*-P[VBTMA][Cl] ionomers (Scheme 2). Quantitative conversion of benzyl chloride units into BTMA salts was confirmed through FTIR spectroscopy by observing the complete disappearance of the C−Cl stretching band at 674 cm^{-1} and C−H wagging band at 1265 cm^{-1} of the chloromethyl group after quaternization (Figure S2). The IEC of the quaternized copolymers was thus easily calculated from the copolymer composition (Table 1).

Quaternization reactions were performed in aqueous TMA solution. Initially, PI-*ran*-PVBCl precursor copolymers formed a heterogeneous slurry with aqueous TMA. During the quaternization process a transition from heterogeneous to homogeneous solution was observed as PI-*ran*-PVBCl copolymers were converted into PI-*ran*-P[VBTMA][Cl] ionomers. This observation was a qualitative confirmation of successful quaternization. Formation of the BTMA provided sufficient hydrophilic character to the PI-*ran*-P[VBTMA][Cl] ionomers to render them water-soluble. All of the quaternized copolymers showed excellent solubility in methanol and ethanol as well, regardless of their IECs, providing solvent processability and facile membrane fabrication. Moreover, this solvent processability, similar to Nafion, potentially allows PI-*ran*-P[VBTMA][Cl] ionomers to be infused into the catalyst layers of membrane electrode assembly for high performance fuel cells. Consequently, PI-*ran*-P[VBTMA][Cl] can serve as both polyelectrolyte membrane and ionomer layer for interfacing with catalysts.

PI-*ran*-P[VBTMA][Cl] ionomers have a polymer backbone similar to the quaternized polystyrene-*block*-poly(ethylene-*ran*-butylene)-*block*-polystyrene (QSEBS). Compared to QSEBS, the preparative process of PI-*ran*-P[VBTMA][Cl] is more environmental friendly due to absence of the toxic chloromethylation step.[25] The composition of PI-*ran*-P[VBTMA][Cl] can be easily tuned by the feeding ratio of the two monomers; high ionic content can be achieved leading to high IEC. While QSEBS membranes were prepared by quaternizing films cast from chlorinated SEBS precursors, solvent processability of PI-*ran*-P[VBTMA][Cl] assures nearly quantitative quaternization and membrane preparation from an ionomer solution.

Membrane Fabrication. It is known that polydienes, such as polyisoprene, undergo complex free radical formation, chain scission, and cross-linking reactions under oxidative conditions, resulting in cross-linked networks.[26,27] This ability to undergo cross-linking was employed to form covalently cross-linked networks from PI-*ran*-P[VBTMA][Cl]-*x* ionomers. Membranes were cast from a methanol solution of the desired PI-*ran*-P[VBTMA][Cl]-*x* ionomer and dried thoroughly. Dry membranes were cross-linked in a preheated oven for a desired time interval. The cross-linking temperature was selected based on thermal gravimetrical analysis (TGA) of the PI-*ran*-P[VBTMA][Cl]-*x* ionomers as shown in Figure 1. The first major weight loss is observed around 200 °C. This is attributed to the decomposition of the TMA groups. Slight weight loss at lower temperatures is presumably due to the loss of trapped water in the highly hygroscopic ionomer. The cross-linking temperature of 145 °C was selected as the highest temperature that would not cause excessive degradation. Since this temperature is slightly above the polymerization temperature, the alkoxyamine end-groups could also be expected to contribute to network formation. After cross-linking robust, water-insoluble membranes were obtained from water-soluble PI-*ran*-P[VBTMA][Cl]-x ionomers.

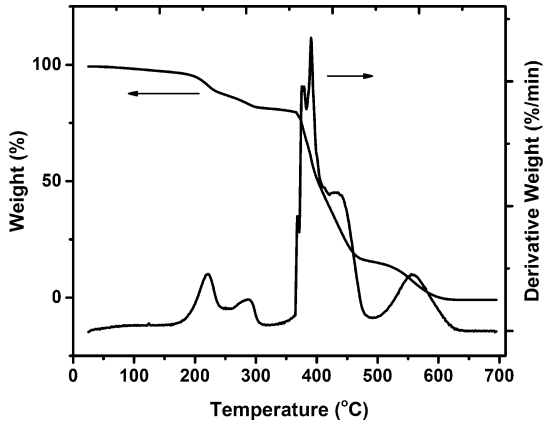

Figure 1. TGA of PI-*ran*-P[VBTMA][Cl]-1.96.

It was observed that cross-linking time had a great influence on ion conductivity. To study the effect of cross-linking time on ion conductivity, five different membranes were prepared from the same precursor (PI-*ran*-P[VBTMA][Cl]-1.96). These membranes were cross-linked for five different time intervals: 3, 6, 12, 24, and 48 h. The highest conductivities were obtained from the membrane that was cross-linked for the shortest time. A monotonic decrease in conductivity was observed with longer cross-linking times (Table S1). For the membrane cross-linked for 48 h the conductivity values were 1 order of magnitude lower than the conductivity of the membrane cross-linked for 3 h. A slight discoloration was also observed with extended cross-linking times, an expected result of oxidative thermal cross-linking. The membranes cross-linked for longer times showed improved dimensional stability. They swelled less when immersed in water compared to the membranes cross-linked for shorter times.

Thermogravimetric analysis was performed to mimic the cross-linking conditions and quantify possible degradation of BTMA groups under elongated cross-linking times. The possible degradation products of BTMA groups, trimethylamine or chloromethane, are volatile organic compounds. Any weight loss during isothermal heating would be presumably due to evaporation of these volatile compounds. The highest IEC ionomer PI-*ran*-P[VBTMA][Cl]-2.34 was used to determine the upper limit of weight loss due to BTMA degradation. The ionomer was heated to 145 °C under air flow for 12 h, and the weight loss at this constant temperature was monitored (Figure S3). The initial weight loss during heating to the isothermal temperature was associated with evaporation of water trapped in the hydroscopic ionomer. The weight loss after 12 h of isothermal heating was determined to be 1.45%. For a material with IEC 2.34 mmol/g a complete degradation of BTMA groups would cause a maximum weight loss around 12.8%. Thus, the IEC of the ionomers is not significantly reduced after elongated cross-linking times.

These findings strongly suggest an increase in cross-link density with elongated cross-linking time. Since these five

DOI: 10.1021/ma502362a
Macromolecules 2015, 48, 655−662

Table 2. PI-*ran*-P[VBTMA][Cl]-*x* Membranes, Cross-Linking Time, Water Uptake, Hydration Number, Conductivity, and Average Distance between Morphological Features

PI-*ran*-P[VBTMA][Cl]-*x*	cross-linking time (h)	WU[a] (wt %)	λ	$\sigma_{60\ °C}$[b] (mS/cm)	$\sigma_{90\ °C}$[b] (mS/cm)	d_{dry}[c] (nm)	d_{wet}[d] (nm)
PI-*ran*-P[VBTMA][Cl]-0.77	3	27.8	20	0.07	0.26	4.7	6.3
PI-*ran*-P[VBTMA][Cl]-1.26	3	114.2	50	9.12	14.0	4.5	5.4
PI-*ran*-P[VBTMA][Cl]-1.54	3	126.9	46	16.8	28.1	4.4	5.0
PI-*ran*-P[VBTMA][Cl]-1.82	6	325.4	99	14.4	28.1	4.2	5.0
PI-*ran*-P[VBTMA][Cl]-2.34	12	515.6	122	12.5	21.2	4.1	5.6

[a]Water uptake. [b]Conductivity measurements are collected at 95% relative humidity. [c]Average distance between ionic clusters as determined from SAXS at 60 °C at dry conditions. [d]Average distance between ionic clusters as determined from SAXS at 60 °C at 95% relative humidity.

membranes were prepared from the same precursor ionomer, they had similar IEC values. Thus, the conductivities of the membranes were presumably affected by the formation of a dense cross-linked network. Formation of a more tortuous conduction path as well as reduced water absorption is expected to slow the ion transport through the membrane. Similar trends have been reported for other cross-linked ion conducting systems.[9,10,12,28]

Knowing that the conductivity can be tuned by altering the cross-linking time, a set of optimized membranes was prepared. A series of low to high IEC membranes were obtained by applying the minimum thermal cross-linking time necessary to yield water insoluble and robust membranes (Table 2). With increasing IEC, hence decreasing isoprene content in the copolymer, longer cross-linking times were found to be necessary to obtain water-insoluble membranes. Membranes with IEC values lower than 1.54 mmol/g were cross-linked for 3 h, while PI-*ran*-P[VBTMA][Cl]-1.82 and PI-*ran*-P[VBTMA][Cl]-2.34 were cross-linked for 6 and 12 h, respectively (Table 2).

Ion Conductivity of PI-*ran*-P[VBTMA][Cl]-*x* Membranes. In-plane conductivity measurements were performed on the optimized series of membranes in the chloride counterion form. Figure 2 demonstrates the conductivities of

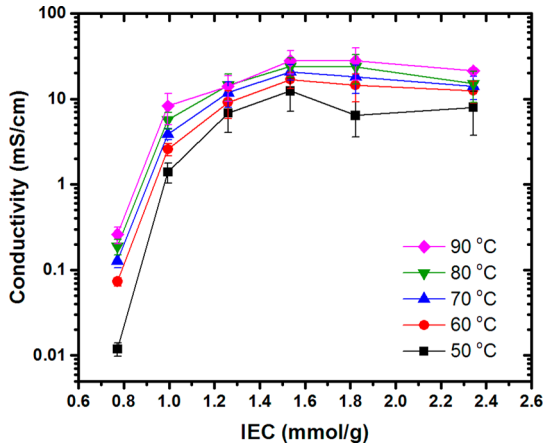

Figure 2. Chloride ion conductivity of PI-*ran*-P[VBTMA][Cl]-*x* membranes as a function of IEC and temperature at 95% RH.

the membranes studied at the temperature range from 50 to 90 °C with respect to their IECs. For fixed IEC, a monotonic increase in ion conductivity is observed with increasing temperature. At constant temperature, conductivity increased with increasing IEC. The most prominent rise in conductivity was detected when IEC was altered from 0.77 to 1.00 mmol/g. A 2 orders of magnitude rise in conductivity was noted for this range. The ion conductivity continues to increase for membranes with IECs up to 1.54 mmol/g. Beyond this initial regime the conductivity values do not increase. For membranes with IECs higher than 1.54 mmol/g, the conductivity values stayed within the same order of magnitude extending to a plateau value. Conductivity values at 60 and 90 °C at 95% relative humidity (RH) are reported in Table 2.

Conductivity properties are closely related to the amount of water absorbed in the membrane, as water forms the necessary medium to facilitate ion transport. Also, conductivity is a function of ion concentration.[29] To understand the conductivity behavior of the membranes, their corresponding water uptake values were measured. Membranes absorbed relatively more water with increasing IEC as an expected result of increased BTMA concentration. For membranes with IECs lower than 1.54 mmol/g moderate water uptake values were observed, while higher IEC membranes absorbed relatively higher amounts of water. This substantial change in water uptake profile beyond a critical IEC value is presumably due to decreasing volume of hydrophobic matrix surrounding the hydrophilic BTMA moieties.

Excessive water uptake is likely the reason for the plateau region for conductivity at high IECs (above 1.54 mmol/g). For ion conducting membranes, it was shown that at sufficiently high hydration levels the diffusion coefficient of ions approach their dilute solution diffusivity limits.[30] Since conductivity is directly proportional to diffusion coefficient of ions, it is expected that the conductivity will reach its highest limit at dilute solution conditions. Thus, high water absorption by PI-*ran*-P[VBTMA][Cl]-1.82 and PI-*ran*-P[VBTMA][Cl]-2.34 membranes presumably causes dilution of chloride ions, resulting in invariant conductivity at IEC increase. A decrease in conductivity with increasing water uptake has been observed previously for BTMA containing polysulfone based anion exchange membranes.[31] These findings suggest that a controlled water uptake is essential to achieve maximum conductivity, while an IEC beyond a certain value might not be necessary for reaching high conductivities.

An accurate measurement of hydroxide ion conductivity under controlled humidities and temperatures is a known challenge.[2,3,31,32] Reactivity of hydroxide ions toward atmospheric carbon dioxide causes formation of a mixture of carbonate, bicarbonate, and hydroxide anions. As a result, an average conductivity is measured. This conductivity is dictated by the relative concentrations of the mixed ions. As mentioned earlier, at high hydration the ion mobility in polymeric media becomes comparable to dilute solution mobilities.[30] It was demonstrated that the ratio between dilute solution mobilities of different ions can be used to estimate the conductivity of a desired ion.[12,31] As discussed above, beyond an IEC of 1.54 mmol/g the conductivity did not change due to dilution of ion

DOI: 10.1021/ma502362a
Macromolecules 2015, 48, 655−662

concentration in the membrane. At dilute solution conditions hydroxide ion mobility is 2.6 times faster than chloride ions. Using this value, hydroxide ion conductivities can be estimated for PI-*ran*-P[VBTMA][Cl]-1.54 and higher IEC membranes.[33] For PI-*ran*-P[VBTMA][Cl]-1.54 these values correspond to 44 mS/cm at 60 °C and 73 mS/cm at 90 °C under 95% RH. These estimated hydroxide conductivities are promising as they are comparable with previously reported conductivity values for cross-linked systems with similar IECs.[11,12,15]

While it is possible to make reasonable estimates using dilute solution mobilities, a 6-fold increase in conductivity upon ion exchange from chloride to hydroxide was reported.[10] It is important to mention that the water uptake profile of membranes may change depending on the counterion, which in turn may affect conductivity. Also, membrane morphology plays a critical role in conductivity properties, and it is important to have a better understanding of the structure–property relationships, as discussed in the following section.

Morphology of Thermally Cross-Linked PI-*ran*-P[VBTMA][Cl]-*x* Membranes. The morphologies of the thermally cross-linked PI-*ran*-P[VBTMA][Cl]-*x* membranes were studied by environmentally controlled SAXS. The scattering curves of the thermally cross-linked membranes were collected at 60 °C under both dry and 95% RH conditions. All membranes displayed a peak indicating microphase separation, both under dry and hydrated environmental conditions (Figure 3). The electron density contrast was

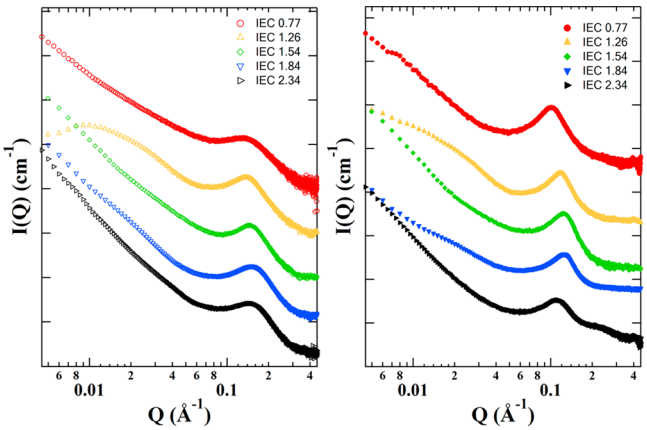

Figure 3. SAXS data for PI-*ran*-P[VBTMA][Cl] copolymers at dry (left) and 95% RH (right) environment. Spectra are offset on *y*-axis for clarity.

obtained from the chloride counterions. Therefore, the scattering features are associated with the existence of ion clusters within the membrane. These scattering peaks are reminiscent of the ionomer peak of hydrated Nafion and correspond to similar average spacing between ion clusters as observed for Nafion.[34−37] The average distances between ion clusters (*d*-spacing) under dry and 95% RH conditions are reported in Table 2.

When dry, the scattering peaks appeared to be broad with low intensities. The breadth and low intensity of the peaks suggest that the scattering features are small and nonuniformly distributed throughout the membrane. The average distances between ion clusters under dry conditions were found to be within the range of 4.7−4.1 nm, decreasing gradually with increasing IEC. This monotonic decrease indicated formation of ion clusters that are closer to each other, presumably due to increasing charge density and decreasing volume of cross-linked matrix surrounding the ion clusters.

With increase of the relative humidity the scattering peaks became more pronounced. The enhanced scattering peak intensity is likely due to enhanced scattering contrast, suggesting formation of well-defined clusters. Relatively sharper scattering peaks compared to the dehydrated state indicated a more uniform *d*-spacing distribution and formation of well-defined segregation of different domains.

Ionomer peaks shifted toward lower scattering angles as the relative humidity of the environment increased. The shift of the scattering peak with increasing humidity confirmed an increase in average *d*-spacing between ionic clusters, suggesting swelling of the membranes induced by water absorption in the hydrophilic domains. This increase is another indication of rearrangement of the ionic groups into well-defined clusters. It has been suggested by Kreuer and colleagues that the morphology of ionomers is dictated by the electrostatic interactions between ionic domains and counter-charged water.[36,38] In other words, the positively charged BTMA groups are ionically bound through water that is negatively charged due to dissociated chloride ions in the aqueous phase. Thus, it can be said that water acts as a binder to keep the positively charged hydrophilic clusters together. As water enters the membrane, ionic clusters rearrange themselves into better-defined domains.

The change in average *d*-spacing for each membrane was analyzed by comparing the difference between the *d*-spacing at dry and hydrated conditions for each IEC. The difference was found to be the largest for the lowest IEC membrane, and the difference decreased gradually until IEC reached 1.54 mmol/g. As discussed earlier, water uptake increases with increasing IEC. As a result, membranes swell and the ionomer peak shifts, as observed in SAXS profiles. Even though the membranes absorb relatively higher amounts of water with increasing IEC, the change in *d*-spacing remains relatively modest. This suggests that there might be an intercluster interaction below a critical average distance that allows formation of an interconnected network of ionic clusters, such that the ionic clusters do not undergo as much rearrangement. The average *d*-spacing between the ionic clusters of PI-*ran*-P[VBTMA][Cl]-0.77 seems to fall outside of this critical distance. This observation suggests that a well-connected network of ionic clusters might have formed beyond a critical IEC (IEC > 0.77 g/mmol).

For higher IEC membranes (IEC > 1.54 mmol/g), the difference in average *d*-spacing starts to broaden. This is presumably related to the greater water uptake at these higher IEC values. The electrostatic interactions between water and the BTMA cations are likely reduced due to screening of the ionic charges. Also, the volume fraction of the hydrophobic network surrounding the hydrophilic cluster is decreased. There is less supporting material to suppress the swelling of the ionic clusters. Thus, the swelling seems to dominate over the mechanical and electrostatic binding forces.

The changes in average *d*-spacing can also be correlated with the conductivity data under similar environmental conditions (60 °C, 95% RH). It can be seen that the average *d*-spacing decreased with increasing IEC for membranes with IECs below 1.54 mmol/g, similar to the trend observed for dry membranes. The decrease in *d*-spacing with increasing IEC is followed by an increase in conductivity. The drop in average *d*-spacing is the largest when IEC is increased from 0.77 to 1.00 mmol/g. For the same IEC transition, the conductivity increase was noted to

DOI: 10.1021/ma502362a
Macromolecules 2015, 48, 655−662

be 2 orders of magnitude. As IEC is increased to 1.26 mmol/g, the change in *d*-spacing is less pronounced, as is the change in conductivity. The substantial increase in conductivity at the lower IEC limits is another strong indication of formation of a better connectivity between the ion clusters. As the distance between ionic clusters becomes smaller, the clusters presumably form a connected network that facilitates ion conduction. The critical distance between ion clusters to form a well-connected ion channel seems to be around 5.0−5.6 nm for the hydrated PI-*ran*-P[VBTMA][Cl]-*x* membranes. These distances lie within the range of previously reported *d*-spacing values for various ion conducting membranes.[37] As proposed early on by Hsu and Gierke for Nafion and as discussed by others,[36,39,40] a percolated network of ion clusters is necessary for ion transport through membranes, while it is not the only factor that provides efficient ion conductivity through polymeric media.

CONCLUSIONS

Copolymers of isoprene and VBCl have been successfully synthesized using the well-known nitroxide-mediated polymerization technique. A wide range of copolymer compositions was achieved. VBCl units were qualitatively quaternized by conversion into BTMA cations, affording solvent processable ionomers over a range of IEC values. Solution-cast membranes were readily thermally cross-linked without the need of additional cross-linkers.

A strong correlation was found between water uptake and conductivity properties; controlled hydration of membranes was found to be essential. Substantial water absorption beyond a critical IEC value and a subsequent drop in conductivity highlighted the importance of the balance between water and ion content in polymeric medium as a design criterion.

Thermally cross-linked membranes showed microphase-separated morphologies that were associated with formation of ionic clusters. Correlation between the characteristic average distance of the ion clusters with water uptake and the conductivity data suggests that water promotes formation of well-defined ionic clusters through electrostatic interactions between BTMA cations and dissociated counterions. A well-connected network of ionic clusters is formed above a critical IEC at average distances of 5.0−5.6 nm. Formation of a percolated network of ion clusters is essential for efficient ion conduction through polymeric medium. This study showed that a balanced relationship between IEC, water absorption, and membrane morphology is necessary to develop AEMs with optimum conductivity properties.

ASSOCIATED CONTENT

Supporting Information

^{1}H NMR of PI-*ran*-PVBCl, FTIR of PI-*ran*-PVBCl precursor before and after quaternization, isothermal TGA, table reporting cross-linking time effect on conductivity. This material is available free of charge via the Internet at http://pubs.acs.org.

AUTHOR INFORMATION

Corresponding Author

*(E.B.C.) E-mail Coughlin@mail.pse.umass.edu.

Author Contributions

T.-H.T. and S.P.E. contributed equally to this work.

Notes

The authors declare no competing financial interest.

ACKNOWLEDGMENTS

Funding was provided by the US Army MURI on Ion Transport in Complex Heterogenous Organic Materials (W911NF-10-1-0520). Use of the Advanced Photon Source, an Office of Science User Facility operated for the U.S. Department of Energy (DOE) Office of Science by Argonne National Laboratory, was supported by the U.S. DOE under Contract DE-AC02-06CH11357.

REFERENCES

(1) Merle, G.; Wessling, M.; Nijmeijer, K. *J. Membr. Sci.* **2011**, *377*, 1−35.
(2) Hickner, M. A.; Herring, A. M.; Coughlin, E. B. *J. Polym. Sci., Part B: Polym. Phys.* **2013**, *51*, 1727−1735.
(3) Varcoe, J. R.; Slade, R. C. T. *Fuel Cells* **2005**, *5*, 187−200.
(4) Varcoe, J. R.; Slade, R. C. T.; Lam How Yee, E. *Chem. Commun.* **2006**, 1428−1429.
(5) Hao, J. H.; Chen, C.; Li, L.; Yu, L.; Jiang, W. *Desalination* **2000**, *129*, 15−22.
(6) Komkova, E.; Stamatialis, D.; Strathmann, H.; Wessling, M. *J. Membr. Sci.* **2004**, *244*, 25−34.
(7) Park, J.-S.; Park, S.-H.; Yim, S.-D.; Yoon, Y.-G.; Lee, W.-Y.; Kim, C.-S. *J. Power Sources* **2008**, *178*, 620−626.
(8) Pan, J.; Chen, C.; Zhuang, L.; Lu, J. *Acc. Chem. Res.* **2012**, *45*, 473−481.
(9) Xiong, Y.; Fang, J.; Zeng, Q. H.; Liu, Q. L. *J. Membr. Sci.* **2008**, *311*, 319−325.
(10) Robertson, N. J.; Kostalik, H. A., IV; Clark, T. J.; Mutolo, P. F.; Abruña, H. D.; Coates, G. W. *J. Am. Chem. Soc.* **2010**, *132*, 3400−3404.
(11) Clark, T. J.; Robertson, N. J.; Kostalik, H. A., IV; Lobkovsky, E. B.; Mutolo, P. F.; Abrun a, H. D.; Coates, G. W. *J. Am. Chem. Soc.* **2009**, *131*, 12888−12889.
(12) Zha, Y.; Disabb-Miller, M. L.; Johnson, Z. D.; Hickner, M. A.; Tew, G. N. *J. Am. Chem. Soc.* **2012**, *134*, 4493−4496.
(13) Price, S. C.; Ren, X.; Jackson, A. C.; Ye, Y.; Elabd, Y. A.; Beyer, F. L. *Macromolecules* **2013**, *46*, 7332−7340.
(14) Kostalik, H. A., IV; Clark, T. J.; Robertson, N. J.; Mutolo, P. F.; Longo, J. M.; Abruña, H. D.; Coates, G. W. *Macromolecules* **2010**, *43*, 7147−7150.
(15) Gu, S.; Cai, R.; Yan, Y. *Chem. Commun.* **2011**, *47*, 2856−2858.
(16) Wang, L.; Hickner, M. A. *Polym. Chem.* **2014**, *5*, 2928.
(17) Schlichting, G. J.; Horan, J. L.; Jessop, J. D.; Nelson, S. E.; Seifert, S.; Yang, Y.; Herring, A. M. *Macromolecules* **2012**, *45*, 3874−3882.
(18) Liu, Y.; Horan, J. L.; Schlichting, G. J.; Caire, B. R.; Liberatore, M. W.; Hamrock, S. J.; Haugen, G. M.; Yandrasits, M. A.; Seifert, S.; Herring, A. M. *Macromolecules* **2012**, *45*, 7495−7503.
(19) Nicolas, J.; Guillaneuf, Y.; Lefay, C.; Bertin, D.; Gigmes, D.; Charleux, B. *Prog. Polym. Sci.* **2013**, *38*, 63−235.
(20) Lacroix-Desmazes, P.; Delair, T.; Pichot, C.; Boutevin, B. *J. Polym. Sci., Part A: Polym. Chem.* **2000**, *38*, 3845−3854.
(21) Harrisson, S.; Couvreur, P.; Nicolas, J. *Macromolecules* **2011**, *44*, 9230−9238.
(22) Benoit, D.; Harth, E.; Fox, P.; Waymouth, R. M.; Hawker, C. J. *Macromolecules* **2000**, *33*, 363−370.
(23) Keoshkerian, B.; Georges, M.; Quinlan, M.; Veregin, R.; Goodbrand, B. *Macromolecules* **1998**, *31*, 7559−7561.
(24) Greenley, R. Z. Q and e Values for Free Radical Copolymerizations of Vinyl Monomers and Telogens. In *Polymer Handbook*; Brandrup, J., Immergut, E. H., Grulke, E. A., Eds.; John Wiley & Sons, Inc.: New York, 1999.
(25) Zeng, Q. H.; Liu, Q. L.; Broadwell, I.; Zhu, A. M.; Xiong, Y.; Tu, X. P. *J. Membr. Sci.* **2010**, *349*, 237−243.
(26) Bussière, P.-O.; Gardette, J.; Lacoste, J.; Baba, M. *Polym. Degrad. Stab.* **2005**, *88*, 182−188.
(27) Alam, T. M.; Celina, M.; Assink, R. A.; Clough, R. L.; Gillen, K. T.; Wheeler, D. R. *Macromolecules* **2000**, *33*, 1181−1190.

DOI: 10.1021/ma502362a
Macromolecules 2015, 48, 655−662

(28) Jeong, M.-H.; Lee, K.-S.; Lee, J.-S. *Macromolecules* **2009**, *42*, 1652−1658.
(29) Hickner, M. A. *J. Polym. Sci., Part B: Polym. Phys.* **2012**, *50*, 9−20.
(30) Disabb-Miller, M. L.; Johnson, Z. D.; Hickner, M. A. *Macromolecules* **2013**, *46*, 949−956.
(31) Yan, J.; Hickner, M. A. *Macromolecules* **2010**, *43*, 2349−2356.
(32) Tsai, T.-H.; Maes, A. M.; Vandiver, M. A.; Versek, C.; Seifert, S.; Tuominen, M.; Liberatore, M. W.; Herring, A. M.; Coughlin, E. B. *J. Polym. Sci., Part B: Polym. Phys.* **2013**, *51*, 1751−1760.
(33) Vanysek, P. Ionic Conductivity and Diffusion at Infinite Dilution. In *CRC Handbook of Chemistry and Physics*, 81st ed.; CRC Press: Boca Raton, FL, 2001.
(34) Schmidt-Rohr, K.; Chen, Q. *Nat. Mater.* **2008**, *7*, 75−83.
(35) Mauritz, K. A.; Moore, R. B. *Chem. Rev.* **2004**, *104*, 4535−4585.
(36) Kreuer, K. D.; Portale, G. *Adv. Funct. Mater.* **2013**, *23*, 5390−5397.
(37) Beers, K. M.; Balsara, N. P. *ACS Macro Lett.* **2012**, *1*, 1155−1160.
(38) Marino, M. G.; Melchior, J. P.; Wohlfarth, A.; Kreuer, K. D. *J. Membr. Sci.* **2014**, *464*, 61−71.
(39) Hsu, W. Y.; Gierke, T. D. *J. Membr. Sci.* **1983**, *13*, 307−326.
(40) Peckham, T. J.; Holdcroft, S. *Adv. Mater.* **2010**, *22*, 4667−4690.

DOI: 10.1021/ma502362a
Macromolecules 2015, 48, 655−662